Applied Clay Science 247 (2024) 107217

Contents lists available at ScienceDirect

Applied Clay Science

journal homepage: www.elsevier.com/locate/clay

Research Paper

Coating of silk sutures by Halloysite/wax Pickering emulsions for controlled delivery of eosin

Lorenzo Lisuzzo [a], Giuseppe Cavallaro [a,b,*], Stefana Milioto [a,b], Giuseppe Lazzara [a,b]

[a] Dipartimento di Fisica e Chimica, Università degli Studi di Palermo, Viale delle Scienze, pad. 17, 90128 Palermo, Italy
[b] Consorzio Interuniversitario Nazionale per la Scienza e Tecnologia dei Materiali, INSTM, Via G. Giusti, 9, I-50121 Firenze, Italy

ARTICLE INFO

Keywords:
Halloysite nanotubes
Wax
Pickering emulsions
Silk sutures
Controlled release

ABSTRACT

Pickering emulsions based on wax and halloysite clay nanotubes have been proposed for the coating treatment of silk sutures with the aim to increase their loading capacity towards eosin, which is an antimicrobial molecule. Moreover, the presence of halloysite/wax microspheres onto the surface of silk sutures has been explored for the controlled release of the hydrophobic drug in aqueous medium at pH = 5.2. In addition, we have studied the influence of the coating on the thermal and mechanical properties of the sutures. As concerns the thermal characteristics, we have performed thermogravimetric experiments to investigate the decomposition of the coated silk as well as their water content, while Differential Scanning Calorimetry has been carried out to study the melting process of wax. Dynamic Mechanical Analysis (DMA) has been employed to determine both the tensile and viscoelastic properties of the sutures. In particular, the viscoelastic features have been investigated at variable temperatures (up to 250 °C) to determine the effects of the wax/Hal microparticles on the glass transition of silk fibroin. In conclusion, this paper demonstrates that the wax/halloysite Pickering emulsions can be successfully employed to generate hydrophobic microdomains onto the surface of silk sutures, which present enhanced flexibility and improved loading capacity towards eosin.

1. Introduction

Pickering emulsions are composed of two immiscible liquids, where one is dispersed into the other, stabilized by interfacially active solid particles (Pickering, 1907; Ramsden, 1904). Since the first studies, by Pickering and Ramsden, Pickering emulsions attracted the attention of the scientific community for their features (Owoseni et al., 2022; Sieben et al., 2022; Destribats et al., 2014). It is well known that two immiscible phases can form a colloidally unstable system that tend to coalesce and separate due to the high surface energy (Arditty et al., 2003). In conventional emulsions, surfactants are used to decrease the surface tension and to provide stabilization. In the case of Pickering emulsions, instead, the attachment of solid particles at the interface creates a physical barrier and provides steric hindrance thus preventing aggregation, ripening and phase separation (Binks, 2002).

The choice of solids can take into account different parameters (e.g. chemistry, morphology, wettability, eco- and bio-compatibility, cost) resulting in a plethora of platforms that can be designed with tailored properties (Marku et al., 2012; Low et al., 2020). Among them, halloysite is a good candidate as Pickering stabilizer.

Halloysite Nanotubes (Hal) are natural aluminosilicates, structurally composed by the alternation of a Si-O-Si tetrahedral layer and an Al-OH octahedral layer (Abdullayev and Lvov, 2013; Lisuzzo et al., 2023). Due to the presence of interlayer water molecules, the resulting sheet tends to roll up in a nanotubular shape, which is a prominent property (Zhang et al., 2019; Sadjadi, 2020). The different chemistry between the external silicic surface and the inner aluminols bearing surface is responsible for the different charge (Duce et al., 2015; Gorrasi, 2015). For instance, the former is negative and the latter is positive in the 2–8 pH range, thus enabling the selective functionalization by electrostatic interactions or covalent bonding (Zhao et al., 2018; Zhang et al., 2019; Caruso et al., 2023). The possibility to tune the surface properties, together with their mechanical strength, biocompatibility and environmental friendliness are requested properties for using inorganic particles in Pickering emulsions (Zhou et al., 2015; Liu et al., 2021; Lisuzzo et al., 2022a). It is worth to note that the tubular morphology, which can be approximated as a solid cylindrical geometry with flat faces, is one of the most efficient for the stabilization of droplets due to a high value of detachment energy (Saha et al., 2013). Moreover, halloysite is a suitable nanoclay for numerous pharmaceutical and biomedical applications,

* Corresponding author at: Dipartimento di Fisica e Chimica, Università degli Studi di Palermo, Viale delle Scienze, pad. 17, 90128 Palermo, Italy.
E-mail address: giuseppe.cavallaro@unipa.it (G. Cavallaro).

https://doi.org/10.1016/j.clay.2023.107217
Received 3 July 2023; Received in revised form 24 October 2023; Accepted 18 November 2023

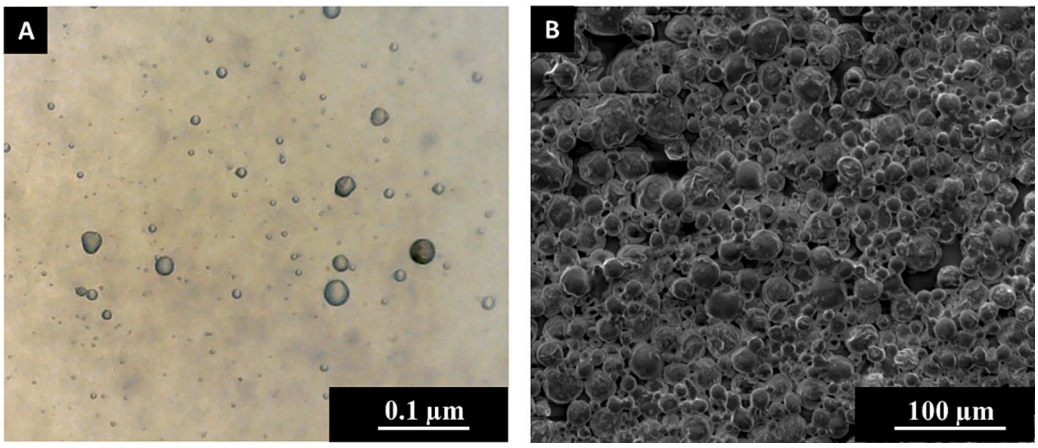

Fig. 1. Optical images (a) and scanning electron microscopy images (b) of the wax/Hal Pickering emulsions.

including tissue engineering (Liu et al., 2013; Huang et al., 2017; Naumenko and Fakhrullin, 2019; Suner et al., 2019) and drug delivery systems (Fizir et al., 2018; Yamina et al., 2018).

Literature reports that an interconnected network of halloysite nanotubes is formed at the fluid interface, which promote reorganization in a radial side-to-side configuration and enhances stability (Kpogbemabou et al., 2014; Stehl et al., 2020). Halloysite based Pickering emulsions have been investigated for environmental purposes (Eskhan et al., 2019; Yu et al., 2019; Panchal et al., 2020), oil recovery (Zhao et al., 2021), catalysis (Stehl et al., 2019), health science (Rezwan et al., 2006), cultural heritage conservation and for improving the properties of building materials (Caruso et al., 2021; Lisuzzo et al., 2021a; Calvino et al., 2022).

Owoseni et al. reported about the design of Hal stabilized droplets by exploiting surfactants loaded nanotubes as efficient protocol for oil spill remediation (Owoseni et al., 2014). Panchal et al. investigated the growth of hydrocarbonoclastic bacteria on oil/seawater emulsions stabilized by halloysite to treat oil spill by bio-remediation (Panchal et al., 2018). Also, halloysite based Pickering emulsions were investigated for the hydroformylation of olefins and for the design of heterogeneous catalysts (von Klitzing et al., 2016). Wei et al. reported the preparation of ibuprofen loaded microparticles by Hal stabilized emulsions as drug delivery systems (Wei et al., 2012). In our previous work, paraffin-in-water emulsions with halloysite were designed for the treatment of waterlogged archeological woods (Lisuzzo et al., 2021b). Similarly, a Pickering emulsions system based on halloysite and on pectin was investigated for the removal of wax from marble surfaces (Cavallaro et al., 2019).

In this work, the preparation of Pickering emulsions is the first step to develop a new class of suture threads that can be used in medical technology.

A suture is a common surgical instrument used to facilitate wound healing by approximating tissues or ligating blood vessels (Lee et al., 2021). The types of sutures can be classified by considering the material (natural or synthetic), the structure (mono- or multi-filament) and the biodegradability (adsorbable or non-adsorbable) (Wancura et al., 2023). Usually, non-adsorbable sutures are required for external wounds because they can be removed through a second procedure (de la Harpe et al., 2021). However, their use can cause additional scar tissue formation and inflammation, which is far from ideal conditions (Ye et al., 2021). Therefore, sutures materials with improved safety and efficacy without lacking biocompatibility are needed (López-Saucedo et al., 2018). Literature reports about coating with functional particles, such as silver and zinc, to enhance the antibacterial properties and to deal with clinical pathogens (De Simone et al., 2014; Thapa et al., 2017; Cao et al., 2019).

In this work, we moved a step forward by treating commercial silk threads with eosin loaded Hal/wax microparticles from Pickering emulsification. Since eosin displays antiseptic and antifungal properties, the resulting material represents an interesting alternative to conventional sutures, with several advantages in terms of mechanical properties, stability and prevention of surgical infections.

2. Experimental

2.1. Materials

Halloysite nanotubes (Hal) ($Al_2Si_2O_5(OH)_4{\cdot}2H_2O$) were purchased from I-Minerals Inc. The suture thread is a Silkam® DS-19 (braided silk – wax and silicone coated) 2/0 USP provided by B-BRAUN (B. Braun Surgical, S.A.). Eosin (2 wt%) was purchased from Nova Argentia Pharmaceutical Industry S.r.l. (Italy). The microcrystalline wax (melting point from 45 to 58 °C) used for the preparation of Pickering emulsion, Sodium Acetate Buffer Solution, (pH = 5.2 ± 0.1) and Sodium Chloride are Sigma Aldrich products.

2.2. Preparation of wax/Hal Pickering emulsions

The preparation of Pickering emulsions was conducted as reported in literature (Lisuzzo et al., 2021a). Briefly, paraffin wax 0.25 wt% was added to hot water (90 °C) under stirring. After complete melting, halloysite was added at 1 wt% and the dispersion was subjected to hot ultrasounds for 10 min and to hot stirring for 30 min. Then, the heating was stopped to allow cooling down. The resulting emulsions were creamy white and did not separate for 7 days at room conditions. Fig. 1 reports the optical and scanning electron microscopy images of wax/Hal emulsions possessing an average diameter of ca. 15–25 µm, in good agreement with literature (Lisuzzo et al., 2021a).

It should be evidenced that Hal acts as emulsifying agent able to stabilize wax (oil phase) in aqueous medium. Namely, halloysite nanotubes are located at the interface of wax droplets driving to obtain stable oil/water Pickering emulsions.

2.3. Sutures impregnation

The impregnation of Silkam® DS-19 suture was carried out by dipping in the wax/Hal Pickering emulsions system at 70 °C. Immersion lasted 15 min, under stirring. Then, the silk sutures were dried at room temperature, washed with water to remove any excess, and dried again prior to further analysis. For comparison, Silkam® DS-19 suture was treated through 1 wt% Hal aqueous dispersion using the same procedure previously described for wax/Hal Pickering emulsions. Based on thermogravimetric experiments, we estimated that the amount of HNTs anchored on the surface is 0.7 wt%. This result is ca. 5 times lower than

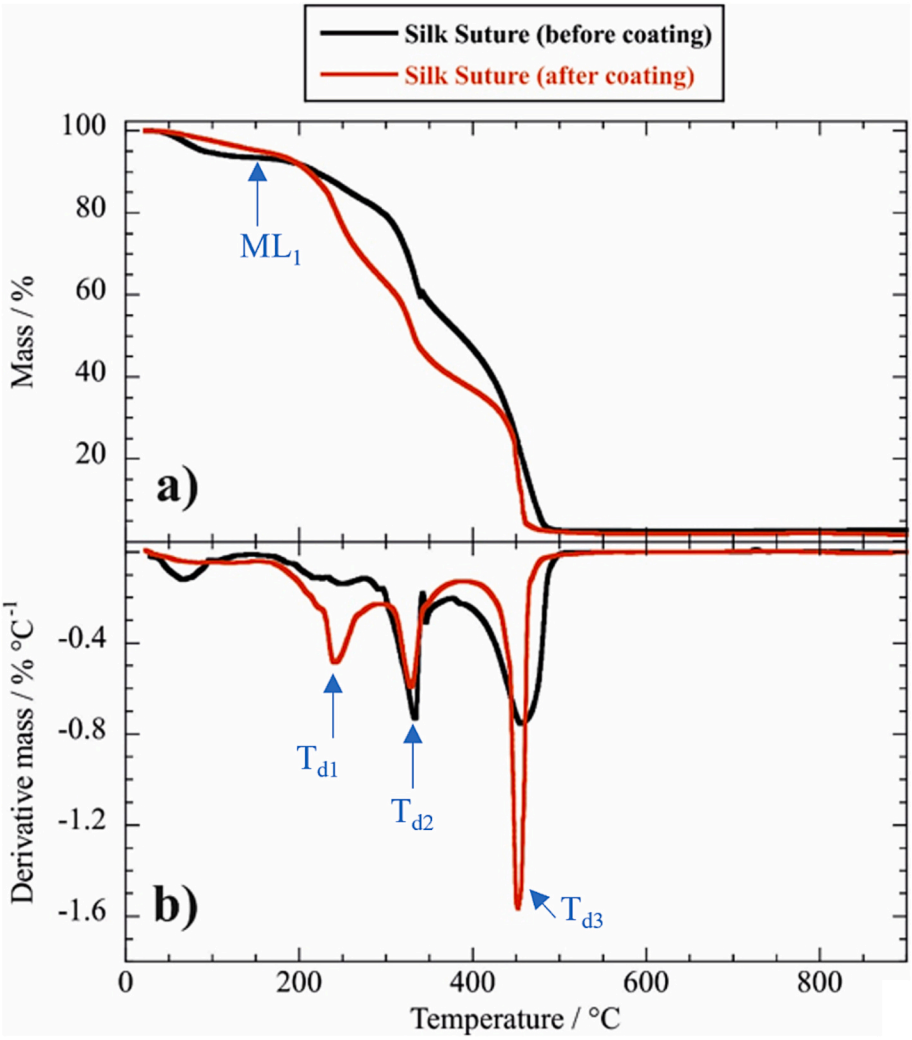

Fig. 2. TG (a) and DTG (b) curves of silk sutures before and after the coating by wax/Hal.

that detected for Hal/wax microparticles.

2.4. Suture impregnation in eosin loaded wax/Hal Pickering emulsions

In order to coat the silk sutures with eosin loaded Pickering emulsions, eosin 2 wt% was added to 10 g of the emulsions and the system was heated up to 70 °C. At this point, the same procedure as for impregnation without eosin was carried out. The sutures were dipped for 15 min, dried and washed with water. For comparison, Silkam® DS-19 was also treated with a solution of eosin 2 wt%, without any Pickering emulsions addition. The same procedure was carried out (heating, drying, washing). These samples were used to investigate the effect of Pickering emulsions.

2.5. Methods

2.5.1. Scanning electron microscopy

Scanning Electron Microscopy (SEM) was performed by using an ESEM FEI QUANTA 200F microscope. In order to avoid charging under the electron beam, the samples were coated with gold in argon by an Edwards Sputter Coater S150A. Micrographs were taken in high vacuum mode ($< 6 \times 10^{-4}$ Pa) for the simultaneous secondary electron. The beam energy was 10 kV and the working distance was 10 mm.

2.5.2. Optical microscopy

Optical microscopy (OM) was conducted to investigate the formation of Pickering emulsions and the structural organization of treated silk sutures. In the first case, micrographs were produced by an Optika polarizing transmission microscope at room temperature. In the second case, instead, optical images were taken with a DIGITUSs (DA-70351) microscope (ASSMANN Electronic GmbHpe, Lüdenscheid, Germany) and processed by using the Digital Viewer 5.7 software.

2.5.3. Thermogravimetry

Thermogravimetric analysis (TGA) was performed using a Q5000 IR apparatus (TA Instruments) under the nitrogen flow of 25 cm^3 min^{-1} for the sample and 10 cm^3 min^{-1} for the balance. The calibration was conducted according to the Curie temperature of standards (nickel, cobalt, and their alloys) (Blanco et al., 2017; Blanco and Siracusa, 2021). Each sample (ca. 5 mg) was heated from room temperature up to 900 °C with a scanning rate of 20 °C min^{-1}.

2.5.4. Differential scanning calorimetry

Differential Scanning Calorimetry (DSC) was carried out by using a TA Instruments DSC apparatus (2920 CE). The calorimeter was calibrated using the melting enthalpy of standard indium (28.71 J g^{-1}). Each sample (2–4 mg) was subjected to two cycles of heating and two cycles of cooling. At first, the samples were heated from 25 to 120 °C and cooled down from 120 to 25 °C with a rate of 10 °C min^{-1}. Then, they

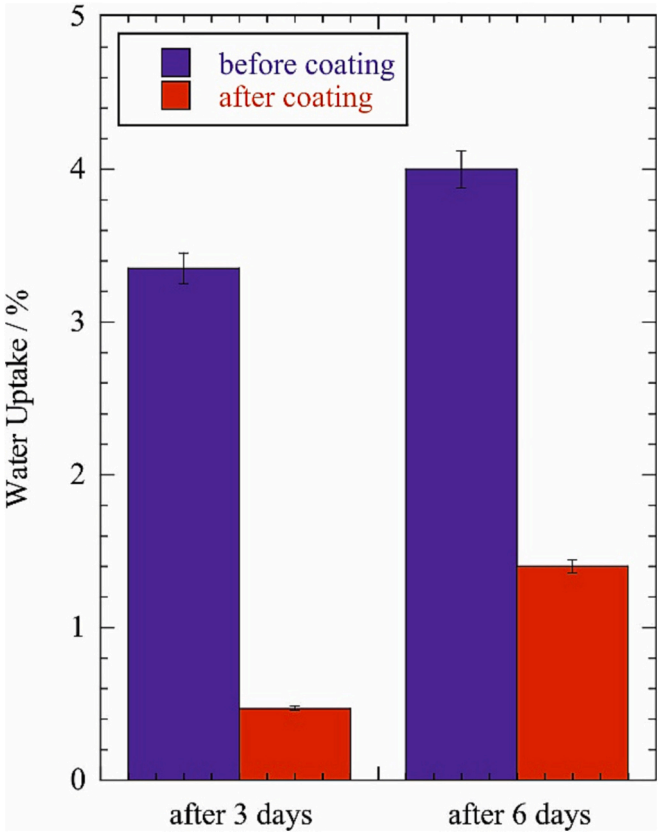

Fig. 3. Water uptake at $R_h = 75\%$ for uncoated and coated silk sutures after 3 and 6 days.

were heated from 25 to 180 °C and cooled down from 180 to 25 °C with the same scanning rate. DSC curves presented in the Results and Discussion section refer to the second heating run. The measurements were performed under a nitrogen flow (rate of 60 cm^3 min^{-1}).

2.5.5. Dynamic mechanical analysis

Dynamic Mechanical Analysis (DMA) was conducted by means of a DMA Q800 instrument (TA Instruments). In particular, the silk sutures were cut in ca. 2 cm long pieces and tensile measurements were performed with a force ramp of 0.5 N min^{-1} at 25.0 ± 0.5 °C. Each sample was measured five times, and the average values with the corresponding errors are reported in Table 3. Moreover, the viscoelastic properties were investigated in the oscillatory regime with a frequency of 1.0 Hz and a strain amplitude of 0.12% by heating the samples from 25 to 250 °C with a rate of 3 °C min^{-1}.

2.5.6. Water uptake

The tests were carried out at a temperature of 25.0 ± 0.5 °C and 75 ± 2% relative humidity (R_h%) using a saturated solution of sodium chloride. The samples were pre-conditioned by drying under vacuum at 25 °C for 2 h and weighed. Then, they were placed in a climate chamber together with a saturated solution of sodium chloride to obtain a stable equilibrium RH%. A thermohygrometer was placed inside the chamber to confirm the environmental parameters. The samples were removed and evaluated by gravimetric analysis at 3 and 6 days using an electronic weighing balance (0.00001 g accuracy). The water uptake (WU %) of the samples was calculated as follows (Caruso et al., 2022):

$$WU(\%) = 100 \bullet (M_t - M_0)/M_0 \quad (1)$$

where M_0 is the initial mass, while M_t is the mass after a certain time of equilibration at the selected RH%.

Table 1
Temperature and mass loss of the different decomposition steps within 180 and 520 °C.

	Decomposition step (180–220 °C)		Decomposition step (220–380 °C)		Decomposition step (380–520 °C)	
	T_{d1} / °C	ML / %	T_{d2} / °C	ML / %	T_{d3} / °C	ML / %
Before coating	243	10.4	335	30.8	457	48.9
After coating	241	26.2	329	27.9	453	37.6

2.5.7. UV–Vis spectrophotometer

The release kinetics of the eosin loaded silk sutures was investigated in sodium acetate buffer (pH = 5.2 ± 0.1) using a UV–Vis spectrophotometer (Specord S600 Analytik Jena). In particular, 1 cm of suture loaded with eosin was placed in the quartz cuvette with 2 ml of buffer solution and spectra were recorded as a function of time by focusing the drug main adsorption band at 515 nm. Prior to measurements, the calibration curve of pure eosin was determined for quantitative analysis. It should be noted that the eosin release was investigated under slightly acidic conditions miming those of human skin, which possess a pH ranging between 5 and 5.5 (He et al., 2023).

3. Results and discussion

3.1. Thermal properties, water uptake and morphology of coated silk sutures

We investigated the effects of the coating by microwax on the thermal characteristics of silk sutures by thermogravimetry and differential scanning calorimetry. Fig. 2a compares the thermogravimetric (TG) curves of the sutures before and after their treatment with the wax/Hal Pickering emulsion.

As a general result, we detected that the TG curves show four distinctive mass losses, which are evident by the peaks of the differential thermogravimetric (DTG) curves (Fig. 2b). The first mass loss (ML_1), which occurs in the range between 25 and 150 °C, reflects the amount of water molecules physically adsorbed onto the sutures (Lisuzzo et al., 2022b). We calculated ML_1 values equal to 6.65 and 4.81 wt% for uncoated and coated sutures, respectively. According to these results, we can state that the presence of microwax reduced the water content of the silk sutures highlighting their hydrophobization. This effect was confirmed by the water uptake values (Fig. 3), which evidenced that coating procedure significantly reduced the capacity of the sutures to absorb water. Specifically, we calculated that the water uptake values decreased by 85 and 65% for sutures kept at $R_h = 75\%$ for 3 and 6 days, respectively.

The thermal decomposition of the main components (silk and wax) of both samples occurred in three steps within the temperature range between 180 and 520 °C. Table 1 reports the decomposition temperatures (taken from the DTG peaks) of the several steps. In general, we observed that the decomposition processes are slightly shifted to lower temperatures after the coating of the sutures. Moreover, we estimated the mass losses related to each step (Table 1).

DSC curves (Fig. 4) of both uncoated and coated sutures showed the presence of an endothermic signal in the range ca. 40–70 °C that could be attributed to the wax melting (Lisuzzo et al., 2021b). In this regard, it should be noted that the uncoated suture possess wax in its composition.

We estimated the temperature of the melting process by the minimum of the DSC peak. Based on this analysis, we observed that the coating procedure reduced the temperature of wax melting. In particular, we calculated that the melting process occurs at 56.4 and 48.2 °C in the uncoated and coated sutures, respectively. Moreover, the integration of the DSC peaks revealed that the melting enthalpy (ΔH_m) is slightly enhanced after the coating in agreement with the incorporation of microwax particles within the silk structure. In detail, we calculated

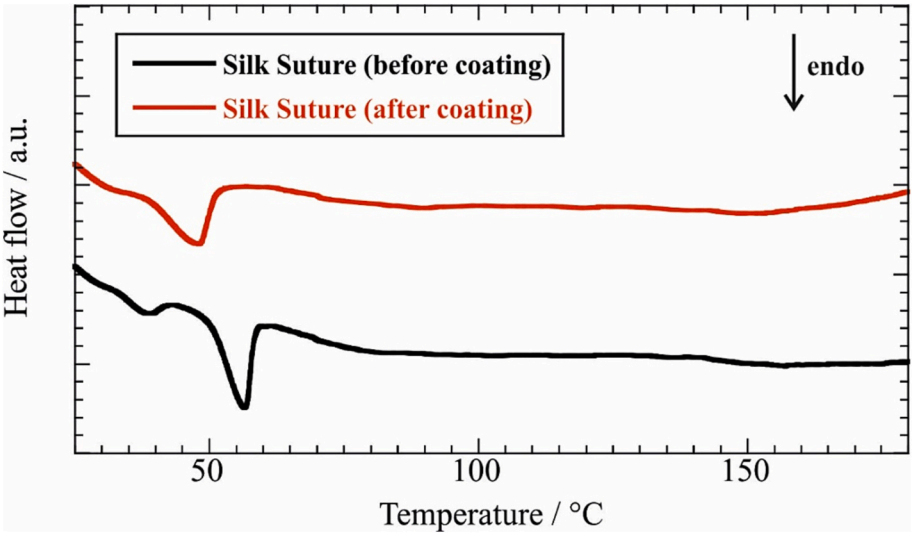

Fig. 4. DSC curves of silk sutures before and after the coating by wax/Hal.

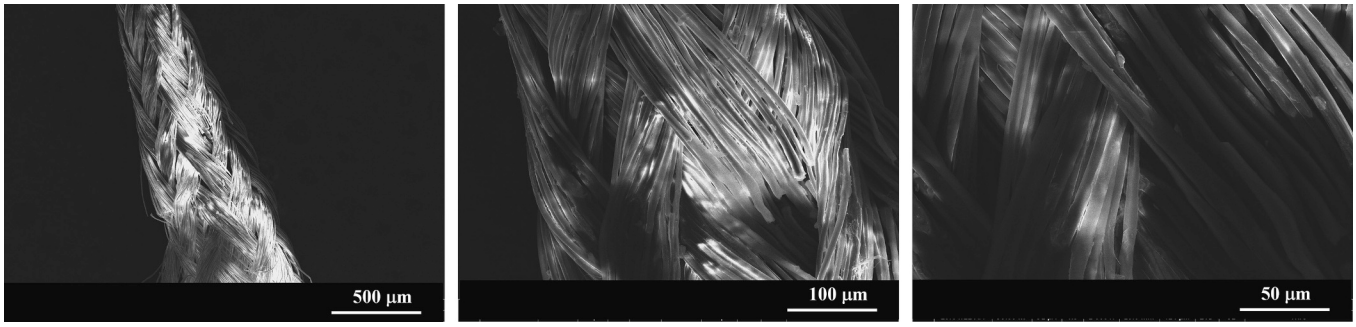

Fig. 5. SEM images of uncoated silk suture.

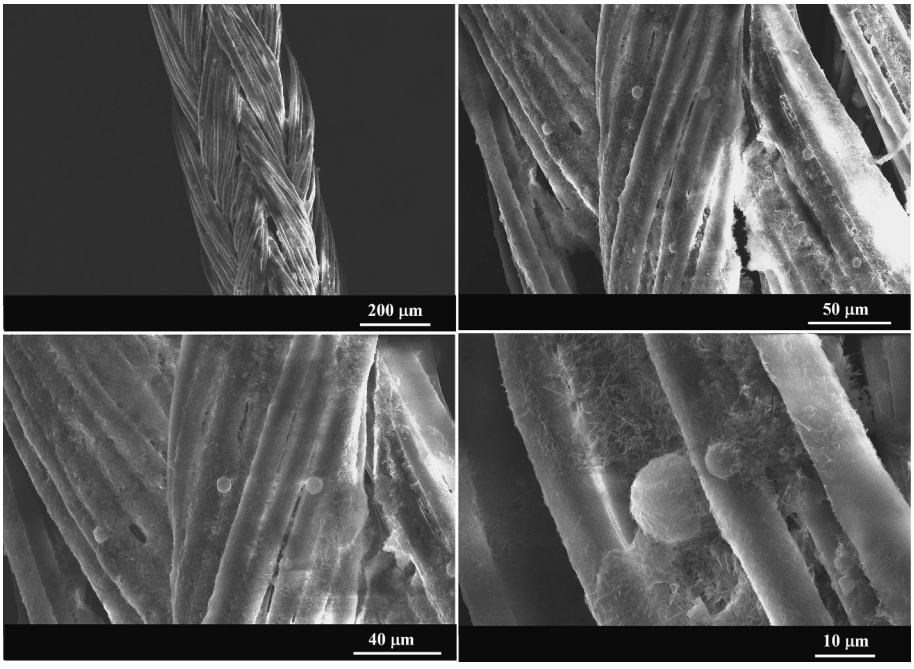

Fig. 6. SEM images of silk suture after the treatment by wax/Hal Pickering emulsion.

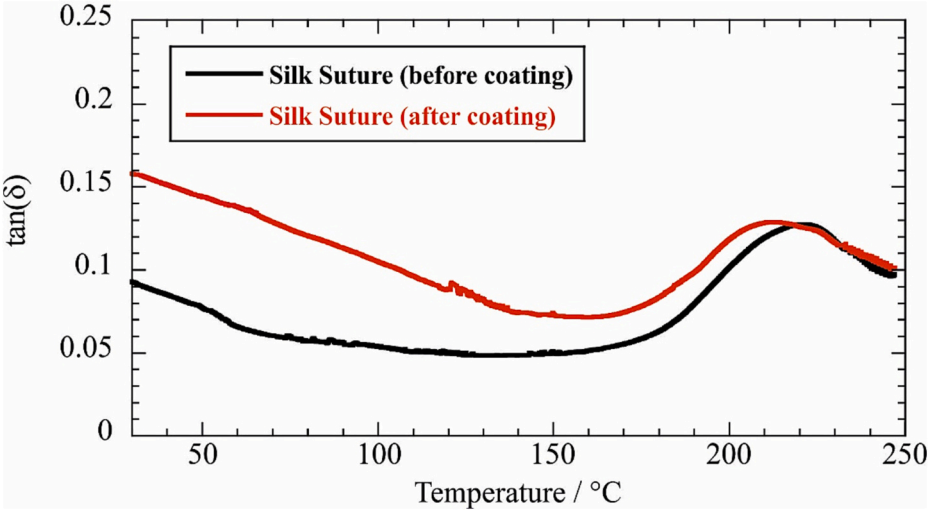

Fig. 7. Tan(δ) vs temperature for uncoated and coated silk sutures.

Table 2
Viscoelastic parameters at 30 °C for uncoated and coated silk sutures.

	G' / MPa	G" / MPa	tan(δ)
Before coating	5250	488	0.0929
After coating	6059	958	0.1581

ΔH_m of 13.7 and 16.5 J g^{-1} for uncoated and coated sutures, respectively.

The morphologies of uncoated and coated silk sutures were investigated by SEM analyses. Fig. 5 shows the untreated suture is composed of multiple filament and its surface does not present any coating particles.

On the other hand, the surface of treated sutures (Fig. 6) presents a random distribution of microwax particles, which possess comparable sizes than those estimated from Fig. 1. It should be noted that clay nanotubes partly cover the interface of the microwax. Besides, a fraction of halloysite is directly anchored onto the surface of the suture.

3.2. Effects of the coating on the mechanical behavior of the silk sutures

DMA experiments were performed on uncoated and coated samples to investigate the effects of microwax on the viscoelastic and tensile properties of silk samples. Regarding the viscoelastic characteristics, we conducted DMA measurements under oscillatory regime within a temperature range between 30 and 250 °C. Fig. 7 shows the dependence of tan(δ) on the temperature for uncoated and coated sutures.

The tan(δ) vs temperature curves of both samples evidenced a peak that can be attributed to the glass transition of silk fibroin in agreement with literature (Guan et al., 2016). We observed that the glass transition is shifted to a lower temperature after the coating of the silk suture. In detail, we calculated glass transition temperatures equal to 221.3 and 211.6 °C for uncoated and coated sutures, respectively, that might be related to an increase of the free volume between the silk fibers due to the presence of wax microspheres. Interestingly, similar results were detected by TGA and DSC, which revealed that the coating treatment induced decreases of the temperatures related to silk thermal decomposition (Fig. 2 and Table 1) and wax melting (Fig. 4).

Moreover, we detected that tan(δ) of the coated suture is larger than that of the uncoated sample for any temperature prior to the silk glass transition (Fig. 7). Being that tan(δ) represents the ratio between G" (loss modulus) and G' (storage modulus), we can state that the coating with microwax enhanced the viscous component of the silk suture. Table 2 reports all the viscoelastic parameters (tan(δ), G' and G") determined at

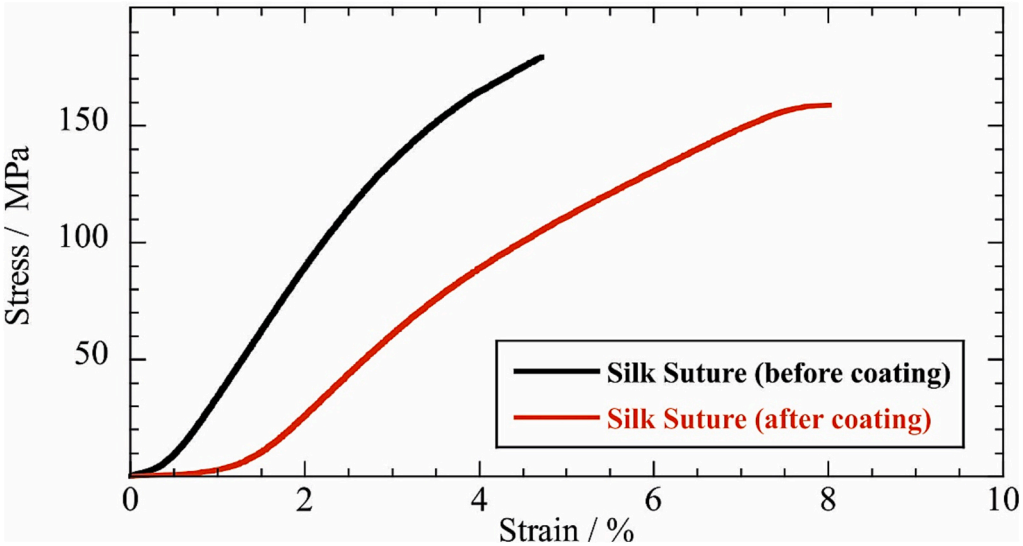

Fig. 8. Stress vs strain curves for silk sutures before and after their coating.

Table 3
Tensile parameters for uncoated and coated silk sutures.

	Stress at break / MPa	Ultimate Elongation / %	Elastic Modulus / MPa
Before coating	179 ± 9	4.74 ± 0.14	5599 ± 405
After coating	158 ± 8	8.0 ± 0.2	3514 ± 250

30 °C for both samples.

Based on the analysis of the stress vs strain curves (Fig. 8), we determined the effects of the microwax addition on tensile properties of the silk sutures.

As shown in Table 3, the coating significantly altered the tensile performances of the sutures.

Compared to the uncoated sample, we observed a slight reduction (ca. 11%) of the stress at break for the treated suture. Oppositely, we detected a relevant enhancement (ca. 69%) of the ultimate elongation after the incorporation of microwax within the silk fibers. Namely, we can state that the presence of wax microspheres increases the flexibility of the silk sutures. According to this consideration, the elastic modulus of the suture was reduced by ca. 59% after its coating (Table 3). The latter agrees with the viscoelastic parameters (Fig. 7 and Table 2), which

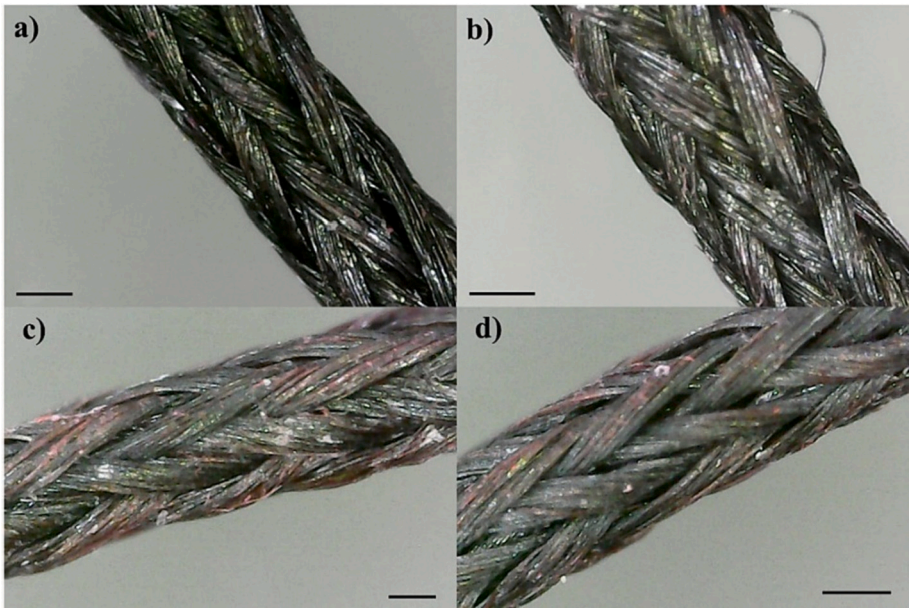

Fig. 9. Optical micrographs of uncoated (a,b) and coated (c,d) silk sutures after their immersion within the eosin solution. The scale bar is 0.1 mm.

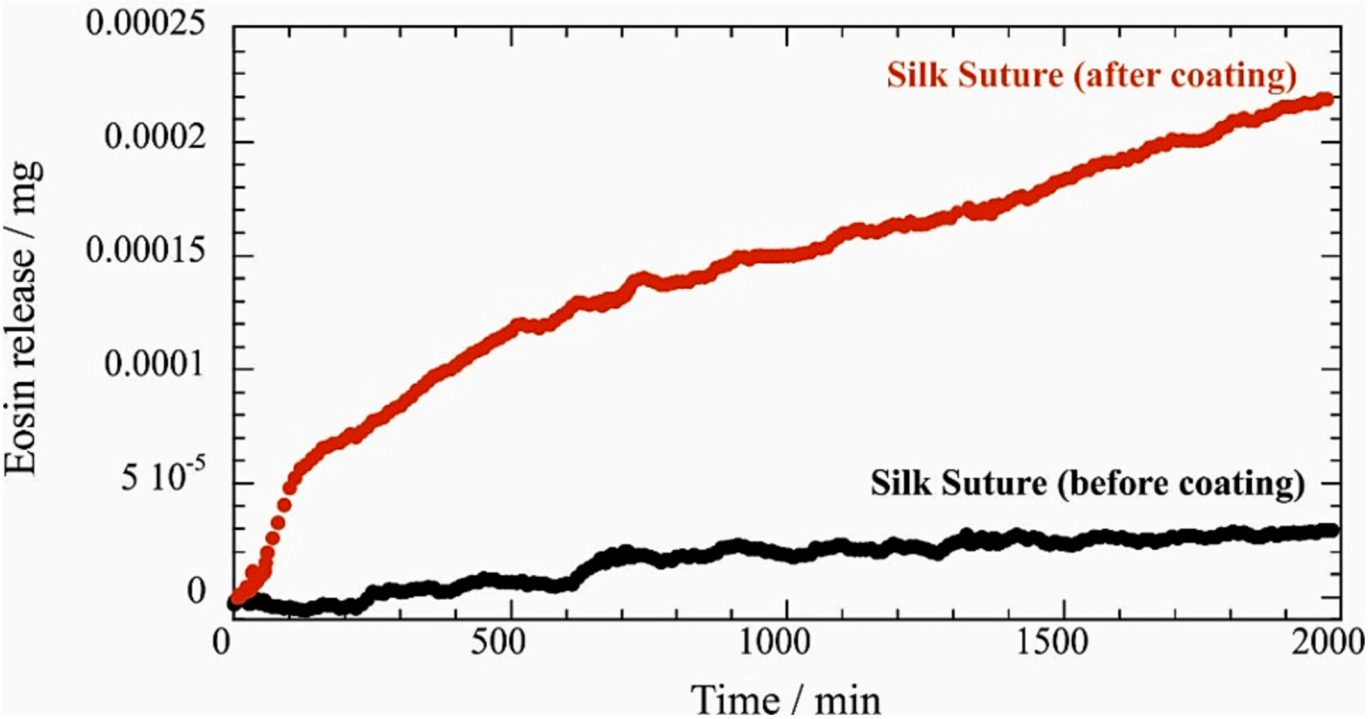

Fig. 10. Release kinetics of eosin from uncoated and coated silk sutures (1 cm of length) in water at pH = 5.2.

evidenced that the elastic contribution decreases after the coating. In conclusion, DMA experiments highlighted that the treatment by wax/Hal Pickering emulsions is effective to obtain flexible silk sutures that preserve a high mechanical resistance to the break.

3.3. Release kinetics of eosin loaded within the coated silk sutures

Fig. 9 shows the optical images of both uncoated and coated silk sutures after their immersion within the eosin solution. Due to the drug loading, the surface of the coated sutures presents a partial reddish coloration, which is not clearly evidenced in the untreated sutures. Namely, we can state that the presence of microwax significantly improved the eosin loading capacity of the suture. This finding indicates that the wax microspheres act as hydrophobic domains with high affinity towards eosin.

We studied the release kinetics of the loaded eosin in aqueous medium at pH = 5.2 by UV–Vis spectroscopy. The released eosin (expressed in mg) vs time profiles are presented in Fig. 10.

According to the optical micrographs, the amount of released eosin is larger for sutures treated by wax/Hal Pickering emulsions. As examples, the eosin released from the coated suture is ca. 0.00022 mg, which is ca. two order of magnitude higher compared to that released from the uncoated sample. We analyzed the release data from the coated suture by the Korsmeyer−Peppas model in order to determine the delivery mechanism from the microwax incorporated within the silk structure. We calculated that the exponential parameter is 0.496 ± 0.008 highlighting that the drug release is based on non Fickian diffusion (Ritger and Peppas, 1987). Accordingly, we can state that the eosin release is governed by diffusion and swelling with similar rates. Literature reports n ≈ 0.5 for the release of Vitamin-D_3 encapsulated within Pickering emulsions formed by zein/chitosan (emulsifying agent) and medium chain triglyceride (oil phase) (Shah et al., 2021). The release of curcumin from cellulose nanocrystals/red palmen oil Pickering emulsions exhibited n values ranging between 0.19 and 0.78 on dependence of the external magnetic field (Low et al., 2019).

Furthermore, the data fitting by Korsmeyer−Peppas equation allowed us to determine the kinetic constant values for eosin release. We detected that the presence of microwax particles decreases the kinetic constant by ca. 2 order of magnitude, Specifically, we calculated kinetic constant values of 52 ± 5 min^{-1} and 0.138 ± 0.012 min^{1} for uncoated and coated sutures, respectively. These results highlighted that wax microspheres stabilize eosin on the suture extending its release over time. This effect could be attributed to the hydrophobic interactions occurring between eosin and microwax.

4. Conclusions

Wax/halloysite Pickering emulsions were successfully employed for the treatment of commercial silk sutures by using an immersion protocol. It should be noted that halloysite acts as emulsifying agent stabilizing wax droplets (oil phase) in water driving to obtain Pickering emulsions. We detected that the coating treatment generated a significant reduction of the water uptake of the silk sutures in agreement with the incorporation of hydrophobic microdomains (the wax/halloysite microspheres) on their structure. SEM images confirmed the presence of randomly distributed microwax particles on the surface of the silk sutures. It should be noted that the wax microspheres on suture surface are partly covered by halloysite clay nanotubes. This finding reflects a reduction of the halloysite ordering due to the suture immersion within Pickering emulsions. Thermogravimetric experiments evidenced that the coated sutures possess a lower amount of physically adsorbed water molecules. TGA and DSC measurements showed a slight decrease of the temperatures for both silk decomposition and wax melting after the coating of the sutures. Compared with the untreated samples, the sutures coated with wax/halloysite microspheres exhibited an improved flexibility as evidenced by the relevant enhancement (ca. 69%) of the ultimate elongation as well as the significant decrease (ca. 59%) of the elastic modulus. According to these results, DMA experiments under oscillatory regime showed that the coating with microwax increases the viscous component of the silk suture. Moreover, these experiments revealed that the glass transition of silk fibroin is shifted to a lower temperature (221.3 and 211.6 °C for uncoated and coated samples, respectively) after the coating treatment. Finally, we used the coated sutures for the loading and controlled release of eosin. Due to the presence of the hydrophobic wax/halloysite microdomains, the coated sutures evidenced a reliable improvement of the loaded eosin. Specifically, we calculated that the loading efficiency increases by ca. two order of magnitude for the coated suture compared to that released from the uncoated sample. Then, we studied the kinetics of the eosin release from the coated suture, which highlighted that this process is driven by non Fickian diffusion according to the Korsmeyer−Peppas model. In conclusion, we demonstrated that the use of wax/halloysite Pickering emulsion can be strategic to extend the applications of a commercial silk sutures because of the improved flexibility and the enhancement of the loading of eosin.

CRediT authorship contribution statement

Lorenzo Lisuzzo: Investigation, Data curation, Writing – original draft. **Giuseppe Cavallaro:** Writing – review & editing, Validation. **Stefana Milioto:** Funding acquisition, Resources. **Giuseppe Lazzara:** Conceptualization, Supervision.

Declaration of Competing Interest

The authors declare that they have no known competing financial interests or personal relationships that could have appeared to influence the work reported in this paper.

Data availability

Data will be made available on request.

Acknowledgments

The work was financially supported by FFR 2023 project and University of Palermo. This work was funded by the European Union (NextGeneration EU) through the MUR-PNRR project SAMOTHRACE (ECS00000022).

References

Abdullayev, E., Lvov, Y., 2013. Halloysite clay nanotubes as a ceramic “skeleton” for functional biopolymer composites with sustained drug release. J. Mater. Chem. B 1, 2894–2903. https://doi.org/10.1039/C3TB20059K.

Arditty, S., Whitby, C.P., Binks, B.P., Schmitt, V., Leal-Calderon, F., 2003. Some general features of limited coalescence in solid-stabilized emulsions. Eur. Phys. J. E: Soft Matter Biol. Phys. 11, 273–281. https://doi.org/10.1140/epje/i2003-10018-6.

Binks, B.P., 2002. Particles as surfactants—similarities and differences. Curr. Opin. Colloid Interface Sci. 7, 21–41. https://doi.org/10.1016/S1359-0294(02)00008-0.

Blanco, I., Siracusa, V., 2021. The use of thermal techniques in the characterization of bio-sourced polymers. Materials 14, 1686. https://doi.org/10.3390/ma14071686.

Blanco, I., Cicala, G., Latteri, A., Saccullo, G., El-Sabbagh, A.M.M., Ziegmann, G., 2017. Thermal characterization of a series of lignin-based polypropylene blends. J. Therm. Anal. Calorim. 127, 147–153. https://doi.org/10.1007/s10973-016-5596-2.

Calvino, M.M., Lisuzzo, L., Cavallaro, G., Lazzara, G., Milioto, S., 2022. Halloysite based geopolymers filled with wax microparticles as sustainable building materials with enhanced thermo-mechanical performances. J. Environ. Chem. Eng. 10, 108594 https://doi.org/10.1016/j.jece.2022.108594.

Cao, F., Zeng, B., Zhu, Y., Yu, F., Wang, M., Song, X., Cheng, X., Chen, L., Wang, X., 2019. Porous ZnO modified silk sutures with dual light defined antibacterial, healing promotion and controlled self-degradation capabilities. Biomater. Sci. 8, 250–255. https://doi.org/10.1039/C9BM01422E.

Caruso, M.R., Megna, B., Lisuzzo, L., Cavallaro, G., Milioto, S., Lazzara, G., 2021. Halloysite nanotubes-based nanocomposites for the hydrophobization of hydraulic mortar. J. Coat. Technol. Res. https://doi.org/10.1007/s11998-021-00522-9.

Caruso, M.R., Lisuzzo, L., Cavallaro, G., Mirto, G., Milioto, S., Lazzara, G., 2022. Thermal and mechanical characterization of yarn samples from flemish tapestry of the

Sixteenth Century. Molecules 27, 8450. https://doi.org/10.3390/molecules27238450.
Caruso, M.R., Cavallaro, G., Milioto, S., Lazzara, G., 2023. Halloysite nanotubes/Keratin composites for wool treatment. Appl. Clay Sci. 238, 106930 https://doi.org/10.1016/j.clay.2023.106930.
Cavallaro, G., Milioto, S., Nigamatzyanova, L., Akhatova, F., Fakhrullin, R., Lazzara, G., 2019. Pickering emulsion gels based on halloysite nanotubes and ionic biopolymers: properties and cleaning action on marble surface. ACS Appl. Nano Mater. 2, 3169–3176. https://doi.org/10.1021/acsanm.9b00487.
de la Harpe, K.M., Kondiah, P.P.D., Marimuthu, T., Choonara, Y.E., 2021. Advances in carbohydrate-based polymers for the design of suture materials: a review. Carbohydr. Polym. 261, 117860 https://doi.org/10.1016/j.carbpol.2021.117860.
De Simone, S., Gallo, A.L., Paladini, F., Sannino, A., Pollini, M., 2014. Development of silver nano-coatings on silk sutures as a novel approach against surgical infections. J. Mater. Sci. Mater. Med. 25, 2205–2214. https://doi.org/10.1007/s10856-014-5262-9.
Destribats, M., Rouvet, M., Gehin-Delval, C., Schmitt, C., Binks, B.P., 2014. Emulsions stabilised by whey protein microgel particles: towards food-grade Pickering emulsions. Soft Matter 10, 6941–6954. https://doi.org/10.1039/C4SM00179F.
Duce, C., Vecchio Ciprioti, S., Ghezzi, L., Ierardi, V., Tinè, M., 2015. Thermal behavior study of pristine and modified halloysite nanotubes. J. Therm. Anal. Calorim. 121, 1011–1019. https://doi.org/10.1007/s10973-015-4741-7.
Eskhan, A., Banat, F., Abu Haija, M., Al-Asheh, S., 2019. Synthesis of mesoporous/macroporous microparticles using three-dimensional assembly of chitosan-functionalized halloysite nanotubes and their performance in the adsorptive removal of oil droplets from water. Langmuir 35, 2343–2357. https://doi.org/10.1021/acs.langmuir.8b04167.
Fizir, M., Dramou, P., Dahiru, N.S., Ruya, W., Huang, T., He, H., 2018. Halloysite nanotubes in analytical sciences and in drug delivery: a review. Microchim. Acta 185, 389. https://doi.org/10.1007/s00604-018-2908-1.
Gorrasi, G., 2015. Dispersion of halloysite loaded with natural antimicrobials into pectins: characterization and controlled release analysis. Carbohydr. Polym. 127, 47–53. https://doi.org/10.1016/j.carbpol.2015.03.050.
Guan, J., Wang, Y., Mortimer, B., Holland, C., Shao, Z., Porter, D., Vollrath, F., 2016. Glass transitions in native silk fibres studied by dynamic mechanical thermal analysis. Soft Matter 12, 5926–5936. https://doi.org/10.1039/C6SM00019C.
He, J., Zhang, Y., Yu, X., Xu, C., 2023. Wearable patches for transdermal drug delivery. Acta Pharm. Sin. B 13, 2298–2309. https://doi.org/10.1016/j.apsb.2023.05.009.
Huang, B., Liu, M., Long, Z., Shen, Y., Zhou, C., 2017. Effects of halloysite nanotubes on physical properties and cytocompatibility of alginate composite hydrogels. Mater. Sci. Eng. C 70, 303–310. https://doi.org/10.1016/j.msec.2016.09.001.
Kpogbemabou, D., Lecomte-Nana, G., Aimable, A., Bienia, M., Niknam, V., Carrion, C., 2014. Oil-in-water Pickering emulsions stabilized by phyllosilicates at high solid content. Colloids Surf. A Physicochem. Eng. Asp. 463, 85–92. https://doi.org/10.1016/j.colsurfa.2014.09.037.
Lee, Y., Kim, H., Kim, Y., Noh, S., Chun, B., Kim, J., Park, C., Choi, M., Park, K., Lee, J., Seo, J., 2021. A multifunctional electronic suture for continuous strain monitoring and on-demand drug release. Nanoscale 13, 18112–18124. https://doi.org/10.1039/D1NR04508C.
Lisuzzo, L., Caruso, M.R., Cavallaro, G., Milioto, S., Lazzara, G., 2021a. Hydroxypropyl cellulose films filled with halloysite nanotubes/wax hybrid microspheres. Ind. Eng. Chem. Res. 60, 1656–1665. https://doi.org/10.1021/acs.iecr.0c05148.
Lisuzzo, L., Hueckel, T., Cavallaro, G., Sacanna, S., Lazzara, G., 2021b. Pickering emulsions based on wax and halloysite nanotubes: an ecofriendly protocol for the treatment of archeological woods. ACS Appl. Mater. Interfaces 13, 1651–1661. https://doi.org/10.1021/acsami.0c20443.
Lisuzzo, L., Cavallaro, G., Milioto, S., Lazzara, G., 2022a. Pickering emulsions stabilized by halloysite nanotubes: from general aspects to technological applications. Adv. Mater. Interfaces 2102346, 1–29. https://doi.org/10.1002/admi.202102346.
Lisuzzo, L., Cavallaro, G., Milioto, S., Lazzara, G., 2022b. Halloysite nanotubes as nanoreactors for heterogeneous micellar catalysis. J. Colloid Interface Sci. 608, 424–434. https://doi.org/10.1016/j.jcis.2021.09.146.
Lisuzzo, L., Bertini, M., Lazzara, G., Ferlito, C., Ferrante, F., Duca, D., 2023. A computational and experimental investigation of the anchoring of organosilanes on the halloysite silicic surface. Appl. Clay Sci. 245, 107121 https://doi.org/10.1016/j.clay.2023.107121.
Liu, M., Wu, C., Jiao, Y., Xiong, S., Zhou, C., 2013. Chitosan-halloysite nanotubes nanocomposite scaffolds for tissue engineering. J. Mater. Chem. B 1, 2078–2089. https://doi.org/10.1039/C3TB20084A.
Liu, L., Pu, X., Tao, H., Chen, K., Guo, W., Luo, D., Ren, Z., 2021. Pickering emulsion stabilized by organoclay and intermediately hydrophobic nanosilica for high-temperature conditions. Colloids Surf. A Physicochem. Eng. Asp. 610, 125694 https://doi.org/10.1016/j.colsurfa.2020.125694.
López-Saucedo, F., Flores-Rojas, G.G., López-Saucedo, J., Magariños, B., Alvarez-Lorenzo, C., Concheiro, A., Bucio, E., 2018. Antimicrobial silver-loaded polypropylene sutures modified by radiation-grafting. Eur. Polym. J. 100, 290–297. https://doi.org/10.1016/j.eurpolymj.2018.02.005.
Low, L.E., Tan, L.T.-H., Goh, B.-H., Tey, B.T., Ong, B.H., Tang, S.Y., 2019. Magnetic cellulose nanocrystal stabilized Pickering emulsions for enhanced bioactive release and human colon cancer therapy. Int. J. Biol. Macromol. 127, 76–84. https://doi.org/10.1016/j.ijbiomac.2019.01.037.
Low, L.E., Siva, S.P., Ho, Y.K., Chan, E.S., Tey, B.T., 2020. Recent advances of characterization techniques for the formation, physical properties and stability of Pickering emulsion. Adv. Colloid Interf. Sci. 277, 102117 https://doi.org/10.1016/j.cis.2020.102117.
Marku, D., Wahlgren, M., Rayner, M., Sjöö, M., Timgren, A., 2012. Characterization of starch Pickering emulsions for potential applications in topical formulations. Int. J. Pharm. 428, 1–7. https://doi.org/10.1016/j.ijpharm.2012.01.031.
Naumenko, E., Fakhrullin, R., 2019. Halloysite nanoclay/biopolymers composite materials in tissue engineering. Biotechnol. J. 14, 1900055. https://doi.org/10.1002/biot.201900055.
Owoseni, O., Nyankson, E., Zhang, Y., Adams, S.J., He, J., McPherson, G.L., Bose, A., Gupta, R.B., John, V.T., 2014. Release of surfactant cargo from interfacially-active halloysite clay nanotubes for oil spill remediation. Langmuir 30, 13533–13541. https://doi.org/10.1021/la503687b.
Owoseni, O., Su, Y., Raghavan, S., Bose, A., John, V.T., 2022. Hydrophobically modified chitosan biopolymer connects halloysite nanotubes at the oil-water interface as complementary pair for stabilizing oil droplets. J. Colloid Interface Sci. 620, 135–143. https://doi.org/10.1016/j.jcis.2022.03.142.
Panchal, A., Swientoniewski, L.T., Omarova, M., Yu, T., Zhang, D., Blake, D.A., John, V., Lvov, Y.M., 2018. Bacterial proliferation on clay nanotube Pickering emulsions for oil spill bioremediation. Colloids Surf. B: Biointerfaces 164, 27–33. https://doi.org/10.1016/j.colsurfb.2018.01.021.
Panchal, A., Rahman, N., Konnova, S., Fakhrullin, R., Zhang, D., Blake, D., John, V., Ivanov, E., Lvov, Y., 2020. Clay nanotube liquid marbles enhanced with inner biofilm formation for the encapsulation and storage of bacteria at room temperature. ACS Appl. Nano Mater. 3, 1263–1271. https://doi.org/10.1021/acsanm.9b02033.
Pickering, S.U., 1907. CXCVI.-Emulsions. J. Chem. Soc. Trans. 91, 2001–2021. https://doi.org/10.1039/CT9079102001.
Ramsden, W., 1904. Separation of solids in the surface-layers of solutions and 'suspensions' (observations on surface-membranes, bubbles, emulsions, and mechanical coagulation).Preliminary account. Proc. R. Soc. Lond. 72, 156–164. https://doi.org/10.1098/rspl.1903.0034.
Rezwan, K., Chen, Q.Z., Blaker, J.J., Boccaccini, A.R., 2006. Biodegradable and bioactive porous polymer/inorganic composite scaffolds for bone tissue engineering. Biomaterials 27, 3413–3431. https://doi.org/10.1016/j.biomaterials.2006.01.039.
Ritger, P.L., Peppas, N.A., 1987. A simple equation for description of solute release I. Fickian and non-fickian release from non-swellable devices in the form of slabs, spheres, cylinders or discs. J. Control. Release 5, 23–36. https://doi.org/10.1016/0168-3659(87)90034-4.
Sadjadi, S., 2020. Halloysite-based hybrids/composites in catalysis. Appl. Clay Sci. 189, 105537 https://doi.org/10.1016/j.clay.2020.105537.
Saha, A., Nikova, A., Venkataraman, P., John, V.T., Bose, A., 2013. Oil emulsification using surface-tunable carbon black particles. ACS Appl. Mater. Interfaces 5, 3094–3100. https://doi.org/10.1021/am3032844.
Shah, B.R., Xu, W., Mráz, J., 2021. Formulation and characterization of zein/chitosan complex particles stabilized Pickering emulsion with the encapsulation and delivery of vitamin D3. J. Sci. Food Agric. 101, 5419–5428. https://doi.org/10.1002/jsfa.11190.
Sieben, P.G., Wypych, F., de Freitas, R.A., 2022. Oleic acid as a synergistic agent in the formation of kaolinite-mineral oil Pickering emulsions. Appl. Clay Sci. 216, 106378 https://doi.org/10.1016/j.clay.2021.106378.
Stehl, D., Milojević, N., Stock, S., Schomäcker, R., von Klitzing, R., 2019. Synergistic effects of a rhodium catalyst on particle-stabilized pickering emulsions for the hydroformylation of a long-chain olefin. Ind. Eng. Chem. Res. 58, 2524–2536. https://doi.org/10.1021/acs.iecr.8b04619.
Stehl, D., Skale, T., Hohl, L., Lvov, Y., Koetz, J., Kraume, M., Drews, A., von Klitzing, R., 2020. Oil-in-water pickering emulsions stabilized by halloysite clay nanotubes toward efficient filterability. ACS Appl. Nano Mater. 3, 11743–11751. https://doi.org/10.1021/acsanm.0c02205.
Suner, S.S., Demirci, S., Yetiskin, B., Fakhrullin, R., Naumenko, E., Okay, O., Ayyala, R. S., Sahiner, N., 2019. Cryogel composites based on hyaluronic acid and halloysite nanotubes as scaffold for tissue engineering. Int. J. Biol. Macromol. 130, 627–635. https://doi.org/10.1016/j.ijbiomac.2019.03.025.
Thapa, R., Bhagat, C., Shrestha, P., Awal, S., Dudhagara, P., 2017. Enzyme-mediated formulation of stable elliptical silver nanoparticles tested against clinical pathogens and MDR bacteria and development of antimicrobial surgical thread. Ann. Clin. Microbiol. Antimicrob. 16, 39. https://doi.org/10.1186/s12941-017-0216-y.
von Klitzing, R., Stehl, D., Pogrzeba, T., Schomäcker, R., Minullina, R., Panchal, A., Konnova, S., Fakhrullin, R., Koetz, J., Möhwald, H., Lvov, Y., 2016. Halloysites stabilized emulsions for hydroformylation of long chain olefins. Adv. Mater. Interfaces 1600435–1600443. https://doi.org/10.1002/admi.201600435.
Wancura, M., Nkansah, A., Chwatko, M., Robinson, A., Fairley, A., Cosgriff-Hernandez, E., 2023. Interpenetrating network design of bioactive hydrogel coatings with enhanced damage resistance. J. Mater. Chem. B. https://doi.org/10.1039/D2TB02825E.
Wei, Z., Wang, C., Liu, H., Zou, S., Tong, Z., 2012. Halloysite nanotubes as particulate emulsifier: Preparation of biocompatible drug-carrying PLGA microspheres based on Pickering emulsion. J. Appl. Polym. Sci. 125, E358–E368. https://doi.org/10.1002/app.36456.
Yamina, A.M., Fizir, M., Itatahine, A., He, H., Dramou, P., 2018. Preparation of multifunctional PEG-graft-halloysite nanotubes for controlled drug release, tumor cell targeting, and bio-imaging. Colloids Surf. B: Biointerfaces 170, 322–329. https://doi.org/10.1016/j.colsurfb.2018.06.042.
Ye, Y., Zhou, Y., Jing, Z., Xu, Y., Yin, D., 2021. Electrospun heparin-loaded nano-fiber sutures for the amelioration of achilles tendon rupture regeneration: in vivo evaluation. J. Mater. Chem. B 9, 4154–4168. https://doi.org/10.1039/D1TB00162K.
Yu, T., Swientoniewski, L.T., Omarova, M., Li, M.-C., Negulescu, I.I., Jiang, N., Darvish, O.A., Panchal, A., Blake, D.A., Wu, Q., Lvov, Y.M., John, V.T., Zhang, D., 2019. Investigation of amphiphilic polypeptoid-functionalized halloysite nanotubes

as emulsion stabilizer for oil spill remediation. ACS Appl. Mater. Interfaces 11, 27944–27953. https://doi.org/10.1021/acsami.9b08623.

Zhang, Y., Bai, L., Cheng, C., Zhou, Q., Zhang, Z., Wu, Y., Zhang, H., 2019. A novel surface modification method upon halloysite nanotubes: a desirable cross-linking agent to construct hydrogels. Appl. Clay Sci. 182, 105259–105267. https://doi.org/10.1016/j.clay.2019.105259.

Zhao, Y., Kong, W., Jin, Z., Fu, Y., Wang, W., Zhang, Y., Liu, J., Zhang, B., 2018. Storing solar energy within Ag-Paraffin@Halloysite microspheres as a novel self-heating catalyst. Appl. Energy 222, 180–188. https://doi.org/10.1016/j.apenergy.2018.04.013.

Zhao, T., Chen, J., Chen, Y., Zhang, Y., Peng, J., 2021. Study on synergistic enhancement of oil recovery by halloysite nanotubes and glucose-based surfactants. J. Dispers. Sci. Technol. 42, 934–946. https://doi.org/10.1080/01932691.2020.1721297.

Zhou, C., Li, H., Zhou, H., Wang, H., Yang, P., Zhong, S., 2015. Water-compatible halloysite-imprinted polymer by Pickering emulsion polymerization for the selective recognition of herbicides. J. Sep. Sci. 38, 1365–1371. https://doi.org/10.1002/jssc.201401469.